

# Dynamic wheelset drive load of the railway vehicle caused by short-circuit motor moment

V. Zeman<sup>a,\*</sup>, Z. Hlaváč<sup>a</sup>

<sup>a</sup>Faculty of Applied Sciences, University of West Bohemia, Univerzitní 22, 306 14 Plzeň, Czech Republic

Received 27 August 2009; received in revised form 7 December 2009

---

## Abstract

The paper deals with mathematical modelling of dynamic response of the railway vehicle wheelset drives caused by short-circuit traction motor torque. The individual wheelset drive with hollow graduated shaft is one of subsystems of the two-axled vehicle bogie with two wheelset drives. The model respects the viscoelastic suspension of the both engine stators with gear housings mounted on the bogie frame and all the other couplings among bogie drive components. The dynamic response is investigated in dependence on longitudinal creepage and forward velocity of the vehicle at the moment of the sudden short-circuit in one asynchronous traction motor. The method is applied to bogie of the electric locomotive developed for speed about 200 km/h by the company ŠKODA TRANSPORTATION, s. r. o. The wheelset drive vibration is confronted with stability conditions of the whole bogie.

© 2009 University of West Bohemia. All rights reserved.

*Keywords:* railway vehicle bogie, short-circuit moment, stability conditions, dynamic load

---

## 1. Introduction

Dynamic properties of individual wheelset drives of railway vehicles are usually investigated using torsional models, as it was shown e.g. in [9, 11]. These models, however, do not enable investigation of dynamic load of wheelset drive components (Fig. 1) affected by spatial vibrations of traction motor (TM), gear housing with gears (G), hollow shaft (H) embracing the wheelset axle and wheelset (W). The spatial vibrations of bogie components affect shaft torques, forces transmitted by gearing, clutches, viscoelastic supports between traction motors with gear housings and the bogie frame (BF) and creep forces acting at the contact patches between rails and wheels. Hence, complex models of railway vehicles or their components, presented e.g. in books [7, 13], in the latest works [6, 10] and there cited papers, were developed. The complex model of the railway vehicle bogie (Fig. 2) with radial, lateral, torsional and bending elastic wheels (Fig. 3) was developed by authors [8] for the purpose of optimization of design parameters in term of dynamic response caused by irregularities of the track geometry and by the polygonalized running surface of the wheels. None of complex and detailed models of the railway vehicle bogie has been used for determination of a dynamic response caused by short-circuit moment in one traction motor.

In this paper the detailed linearized model of the two-axled bogie with two individual wheelset drives is used for investigation of this extreme phenomenon in dependence on operational conditions at the short-circuit instant in one traction motor.

---

\*Corresponding author. Tel.: +420 377 632 332, e-mail: zemanv@kme.zcu.cz.

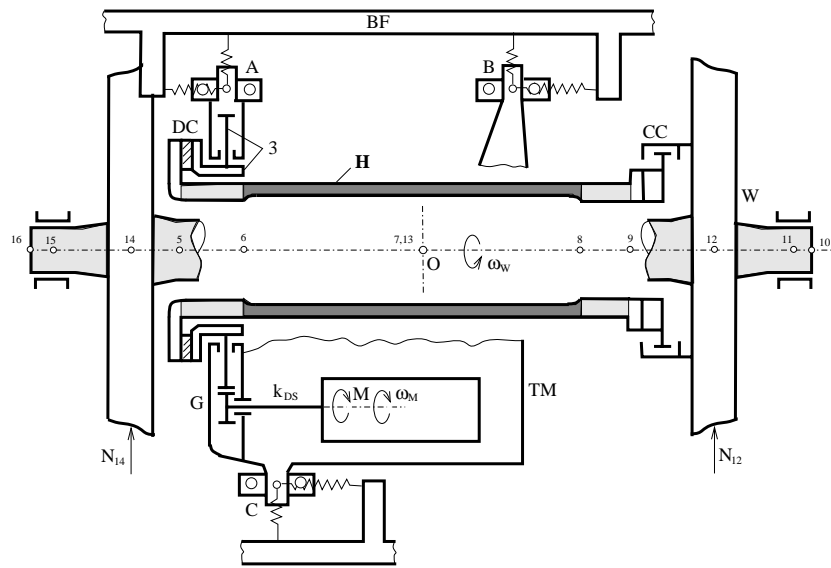


Fig. 1. Scheme of wheelset drive with a hollow shaft

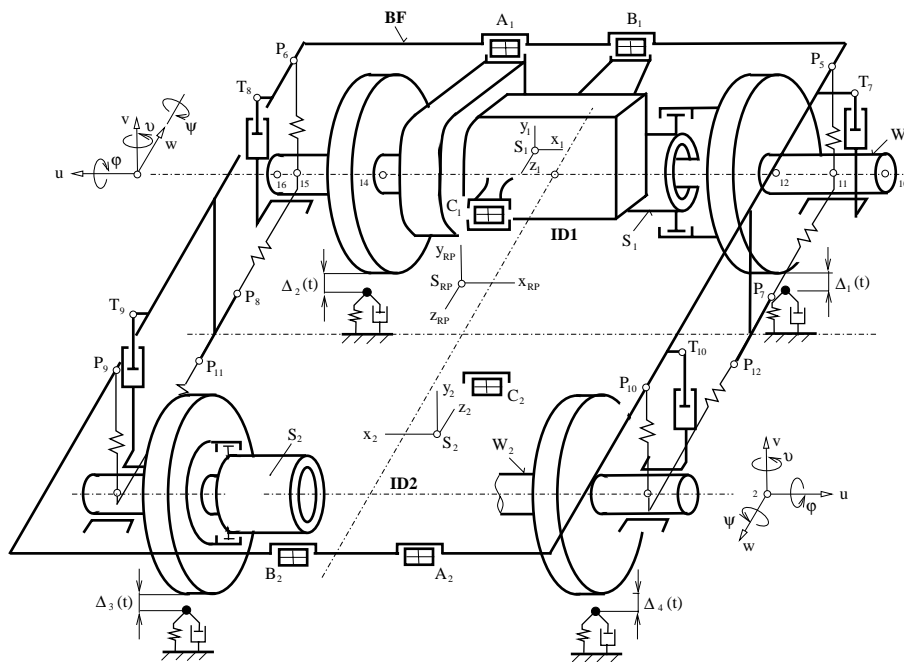


Fig. 2. Scheme of the bogie

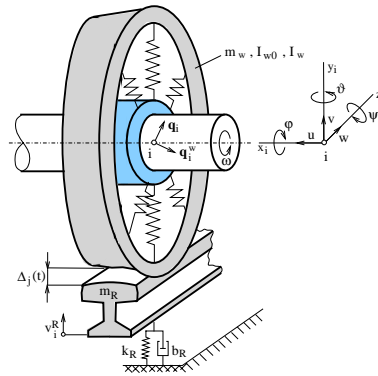


Fig. 3. Scheme of the elastic wheel

## 2. Mathematical model of the bogie

The development of the mathematical model of the bogie with rigid wheels was presented in the paper [15] and detailed in the research report [14]. The mathematical model of the bogie with elastic wheels was derived in configuration space [8]

$$\mathbf{q}(t) = [\mathbf{q}_{ID1}^T(t), \mathbf{q}_{BFCB}^T(t), \mathbf{q}_{ID2}^T(t)]^T \quad (1)$$

of dimension 189, where subvectors correspond to three subsystems – two individual wheelset drives and bogie frame linked by the secondary suspension to a half of the car body. Each individual drive (subscripts ID1 and ID2) is composed from rigid mass components (see Fig. 2) – rotor of traction motor, driving and driver gear, stator of traction motor with gear housing. These components are coupled by massless viscoelastic couplings – driving shaft with torsional stiffness  $k_{DS}$ , gearing with mesh stiffness  $k_G$ , disc clutch (DC) characterized by diagonal stiffness matrix (stiffnesses with one subscript are translational and with double subscript are flexural)

$$\mathbf{K}_{DC} = \text{diag}[k_x, k_y, k_z, k_{xx}, k_{yy}, k_{zz}],$$

rubber silent blocks with centres of elasticity  $A_1, B_1, C_1$  (for ID1) and  $A_2, B_2, C_2$  (for ID2) characterized by translation stiffnesses arranged in diagonal matrix  $\mathbf{K}_{SB} = \text{diag}[k_x, k_y, k_z]$ , disc clutch (DC), claw clutch (CC) with torsional stiffnesses  $k_{DC}$  and  $k_{CC}$  and railway balast (rail, railpad, sleeper and balast) reduced to a single mass-spring-damper system [5] defined by mass, stiffness and damping parameters  $m_R, k_R, b_R$ . The composite hollow shafts and wheelset axes are considered to be one-dimensional continua and are discretized by FEM. Their node displacements are expressed by the vector (see Fig. 2)

$$\mathbf{q}_i = [u_i, v_i, w_i, \varphi_i, \vartheta_i, \psi_i]^T, \quad i = 5, \dots, 16. \quad (2)$$

The rigid discs of clutches, journals and wheels are mounted at nodes  $i = 5$  (DC),  $i = 9$  (CC),  $i = 11, 15$  (journals) and  $i = 12, 14$  (wheels). The flexible connection between the wheel rims and the wheel discs (Fig. 3) can be represented by massless springs and dampers [2]. Each wheel rim may undergo lateral, vertical, longitudinal, torsional, yaw and roll motion described by the displacement vector

$$\mathbf{q}_i^w = [u_i^w, v_i^w, w_i^w, \varphi_i^w, \vartheta_i^w, \psi_i^w]^T, \quad i = 12, 14 \quad (3)$$

for both individual drives ID1 and ID2. Individual drives are placed centrally symmetrical in the bogie. The rigid bogie frame is linked by secondary suspension  $P_1$ – $P_4$  and dampers  $T_1$ – $T_6$  with a half of car body (Fig. 4).

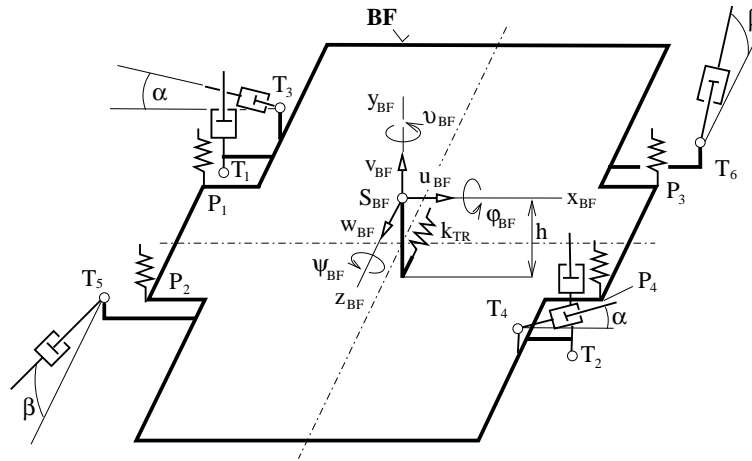


Fig. 4. Model of the bogie frame with the secondary suspension

The mathematical model of the bogie has the form [8]

$$M\ddot{q}(t) + B\dot{q}(t) + Kq = f_G + f_M(\dot{q}, t) + f_{R,W}(q, \dot{q}, t), \quad (4)$$

where matrices have the block-diagonal structure

$$\begin{aligned} M &= \text{diag}[M_{ID}, M_{BF}, M_{ID}], \\ B &= \text{diag}[B_{ID}, B_{BF}, B_{ID}] + B_{D,BF} + B_{W,BF}, \\ K &= \text{diag}[K_{ID}, K_{BF}, K_{ID}] + K_{D,BF} + K_{W,BF} \end{aligned} \quad (5)$$

corresponding to subsystems. Matrices  $B_{D,BF}$  and  $K_{D,BF}$  describe the viscoelastic supports of the stators with gear housings of both traction motors to the bogie frame in silent blocks. Matrices  $B_{W,BF}$  and  $K_{W,BF}$  describe damping and stiffnesses of the primary suspension at points  $T_7$  to  $T_{10}$  (damping) and  $P_5, P_6, P_9, P_{10}$  (stiffness) and the longitudinal wheelset guide between journal boxes and the bogie frame at points  $P_7, P_8, P_{11}, P_{12}$  (see Fig. 2). The vector  $f_G$  expresses all gravitational forces and the vector  $f_M(\dot{q}, t)$  expresses the motor driving torques. The vector  $f_{R,W}(q, \dot{q}, t)$  includes contact forces between rails and wheel rims affected by track or wheel surface deviations  $\Delta_j(t)$ ,  $j = 1, 2, 3, 4$  (see Fig. 2 and Fig. 3).

### 3. Linearized mathematical model of the bogie

To analyze the dynamic response of the bogie caused by the sudden short-circuit for instance in traction motor ID1 we neglect track and wheel irregularities  $\Delta_j(t) = 0$ ,  $j = 1, 2, 3, 4$ . The torque characteristics of the fellow asynchronous traction motor of ID2 is linearized in the neighbourhood of the state before short-circuit

$$M_{ID2} = M(s_0, v) - b_M \Delta \dot{\varphi}_1^{(ID2)}, \quad (6)$$

where  $b_M$  is the slope of the traction motor characteristics and  $\Delta \dot{\varphi}_1^{(ID2)}$  is disturbance angular velocity of the rotor with respect to rotation corresponding to vehicle forward velocity  $v$  and longitudinal creepage  $s_0$  of all wheels. The motor torque of both electric motors in a state of static equilibrium is

$$M(s_0, v) = 2\mu(s_0, v)N_0r_0/p, \quad (7)$$

where  $\mu(s_0, v)$  is longitudinal creep coefficient [11],  $N_0$  is static vertical wheel force,  $r_0$  is wheel radius in central position and  $p = \frac{\omega_M}{\omega_W}$  is speed ratio.

Longitudinal  $T_{iad}$ , lateral  $A_{iad}$  creep forces and spin torque  $M_{iad}$  acting at the contact patches between rails and wheels can be expressed as

$$T_{iad} = \mu(s_i, v)N_i, \tag{8}$$

$$A_{iad} = b_{22}(\dot{u}_i^w + r_i\dot{\psi}_i^w) + b_{23}\dot{v}_i^w, \tag{9}$$

$$M_{iad} = -b_{23}(\dot{u}_i^w + r_i\dot{\psi}_i^w) + b_{33}\dot{v}_i^w, i = 12, 14 \tag{10}$$

for ID1 and ID2. The longitudinal creep force is expressed in dependence on actual longitudinal creep coefficient  $\mu(s_i, v)$  and on vertical wheel force

$$N_i = N_0 - (m_R\ddot{v}_i^w + b_R\dot{v}_i^w + k_Rv_i^w). \tag{11}$$

The longitudinal creep coefficient  $\mu(s_i, v)$  depends on longitudinal creepage defined by

$$s_i = s_0 + \frac{\pm\dot{w}_i^w \mp r_i\Delta\dot{\varphi}_i^w}{v}, s_0 = \frac{r_0\omega_W}{v}, i = 12, 14. \tag{12}$$

whereas upper signs correspond to wheelset  $W_1$  and lower signs to wheelset  $W_2$ , which rotate with angular velocity  $\omega_W$  before the sudden shot-circuit. The vertical wheel forces are expressed in dependence on vertical displacements  $v_i^w$ , velocities  $\dot{v}_i^w$  and accelerations  $\ddot{v}_i^w$  of wheel rim mass centre. The whole track structure (rail, railpad, sleeper and balast) is reduced to a single mass-spring-damper system [5] defined by mass, stiffness and damping parameters  $m_R, b_R, k_R$  figuring in term for  $N_i$ . The lateral creep force and the spin torque about vertical axis depend on linearized creep coefficients  $b_{ij}$ , actual wheel radius  $r_i$  and wheel rim mass centre velocities, marked with subscript  $w$  (see Fig. 3). The creep coefficients were calculated using Kalker’s theory [7] for static vertical wheel force  $N_0$ .

To analyze the modal properties, stability conditions and vibration of the bogie, the longitudinal creep characteristics defined in [3, 12] and presented in Fig. 5 are linearized in the neighbourhood of a state before short-circuit in the form

$$\mu(s_i, v) = \mu_0(s_0, v) + \left[ \frac{\partial\mu}{\partial s_i} \right]_{s_i=s_0} (s_i - s_0). \tag{13}$$

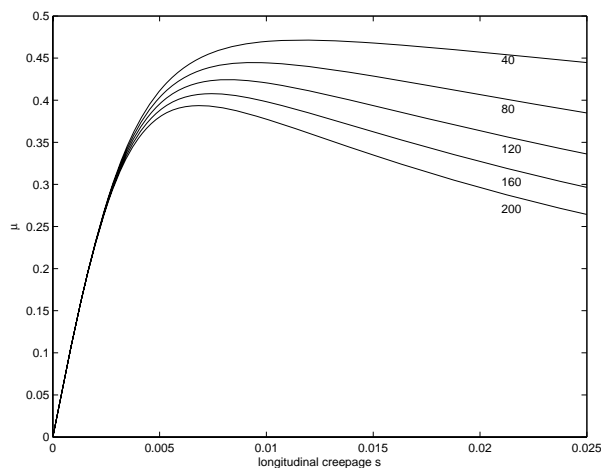


Fig. 5. Creep characteristics

The linearized longitudinal creep forces can be then expressed for  $N_i = N_0$  and  $r_i = r_0$  as

$$T_{iad} = \mu(s_o, v)N_0 + b_{11}(\pm \dot{w}_i^w \mp r_0 \Delta \dot{\varphi}_i^w), \quad i = 12, 14, \quad (14)$$

where

$$b_{11} = \frac{N_0}{v} \left[ \frac{\partial \mu}{\partial s_i} \right]_{s_i=s_0}. \quad (15)$$

If the static equilibrium is disturbed by short-circuit moment  $M_C(t)$  of the traction motor in ID1, the vector of generalized coordinates is expressed as a sum of static and dynamic displacements

$$\mathbf{q}(t) = \mathbf{q}_0 + \Delta \mathbf{q}(t). \quad (16)$$

After expressing of the motor torque in ID2 according (6) and the creep forces according (8) to (15), the force vectors on right side of equation (4) can be written as

$$\mathbf{f}_G + \mathbf{f}_M(\dot{\mathbf{q}}, t) + \mathbf{f}_{R,W}(\mathbf{q}, \dot{\mathbf{q}}, t) = \mathbf{f}_0 - [\mathbf{B}_M + \mathbf{B}_{ad}(s_0, v)]\Delta \dot{\mathbf{q}}(t) + \Delta \mathbf{f}(t). \quad (17)$$

The vector  $\mathbf{f}_0 = \mathbf{K}\mathbf{q}_0$  expresses static force effects before the sudden short-circuit. The diagonal matrix  $\mathbf{B}_M$  has nonzero elements  $b_M$  on positions corresponding to rotor and stator angular velocities of the traction motor of ID2 in vector  $\mathbf{q}(t)$ . The block diagonal matrix of all creep forces

$$\mathbf{B}_{ad}(s_0, v) = \text{diag}[\dots, \bar{\mathbf{B}}_{ad} \dots, \bar{\mathbf{B}}_{ad} \dots, \bar{\mathbf{B}}_{ad} \dots, \bar{\mathbf{B}}_{ad}] \quad (18)$$

has nonsymmetrical blocks

$$\bar{\mathbf{B}}_{ad} = \begin{bmatrix} b_{22} & 0 & 0 & 0 & b_{23} & r_0 b_{22} \\ 0 & 0 & 0 & 0 & 0 & 0 \\ 0 & 0 & b_{11} & -r_0 b_{11} & 0 & 0 \\ 0 & 0 & -r_0 b_{11} & r_0^2 b_{11} & 0 & 0 \\ -b_{23} & 0 & 0 & 0 & b_{33} & -r_0 b_{23} \\ r_0 b_{22} & 0 & 0 & 0 & r_0 b_{23} & r_0^2 b_{22} \end{bmatrix}, \quad (19)$$

which are localized on positions corresponding to wheel rim displacement vectors  $\mathbf{q}_i^w$ , ( $i = 12, 14$  for both wheelsets) in vector of generalized coordinates  $\mathbf{q}(t)$ . The linearized mathematical model of the bogie according (4), (16) and (17) can be written in perturbation coordinates in the neighbourhood of the static equilibrium as

$$M\Delta \ddot{\mathbf{q}}(t) + [\mathbf{B} + \mathbf{B}_M + \mathbf{B}_{ad}(s_0, v)]\Delta \dot{\mathbf{q}}(t) + \mathbf{K}\Delta \mathbf{q}(t) = \Delta \mathbf{f}(t). \quad (20)$$

The excitation (perturbation) vector  $\Delta \mathbf{f}(t)$  has nonzero components  $M_C(t)$  on positions corresponding to angular displacements of the rotor and stator of the traction motor in ID1 in vector of generalized coordinates  $\mathbf{q}(t)$ .

#### 4. Stability conditions of the bogie

The stability conditions of the bogie with rigid wheels were investigated in [15]. In this paper, for the purpose of association with dynamic response caused by short-circuit traction motor, the complex linearized autonomous mathematical model (20) can be used for stability analysis. Eigenvalues are defined by eigenvalue problem solution

$$[\lambda_\nu \mathbf{N}(s_0, v) + \mathbf{P}]\mathbf{u}_\nu = \mathbf{0} \quad (21)$$

in the state space  $\mathbf{u} = [\Delta\dot{\mathbf{q}}^T, \Delta\mathbf{q}^T]^T$ , defined by matrices

$$\mathbf{N}(s_0, v) = \begin{bmatrix} \mathbf{0} & \mathbf{M} \\ \mathbf{M} & \mathbf{B} + \mathbf{B}_M + \mathbf{B}_{ad}(s_0, v) \end{bmatrix}, \mathbf{P} = \begin{bmatrix} -\mathbf{M} & \mathbf{0} \\ \mathbf{0} & \mathbf{K} \end{bmatrix}. \quad (22)$$

The eigenvalues  $\lambda_\nu$  depend on operational parameters  $s_0, v, N_0$  and on the slope  $b_M$  of torque characteristic of the traction motor in ID2 at the instant of the short-circuit in the motor of ID1. In the first step we perform eigenvalue problem solution for different longitudinal creepage  $s_0 = 0.005$  (stable state) and  $s_0 = 0.014$  (unstable state) corresponding to motor torque  $M_0(s_0, v) = 12\,800$  [Nm] for forward vehicle velocity  $v = 120$  [km/h] and  $N_0 = 10^5$  [N].

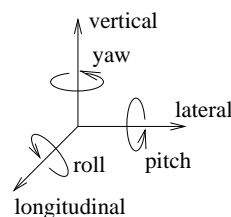
Table 1. Eigenvalues of bogie

eigenvalues sequence	$s_0=0.005, v=120$ km/h		$s_0=0.014, v=120$ km/h	
	complex	real	complex	real
1	$-0.032 \pm i1.262$	$-1.11 \cdot 10^{-11}$	$-0.029 \pm i1.262$	<b>7.031</b>
2	$-0.041 \pm i2.694$	$-2.73 \cdot 10^{-11}$	$-0.060 \pm i2.689$	<b>0.062</b>
3	$-0.199 \pm i5.425$	$-0.0156$	<b>0.076</b> $\pm i5.374$	$-1.17 \cdot 10^{-12}$
4	$-0.056 \pm i5.449$	$-0.0271$	$-0.0318 \pm i5.443$	$-4.36 \cdot 10^{-9}$
5	$-1.583 \pm i6.176$	$-0.0717$	$-1.583 \pm i6.174$	$-0.0158$
6	$-0.164 \pm i8.503$	$-1.611$	$-0.164 \pm i8.505$	$-0.0299$
7	$-0.289 \pm i8.583$	$-1.790$	<b>0.416</b> $\pm i9.126$	$-0.0717$
8	$-3.282 \pm i9.183$	$-5.147$	<b>1.111</b> $\pm i9.535$	$-1.612$
9	$-3.958 \pm i12.208$	$-6.221$	<b>0.911</b> $\pm i12.140$	$-5.438$
10	$-4.010 \pm i12.58$	$-14.521$	<b>0.809</b> $\pm i12.162$	$-6.254$

Table 2. Characteristics of the vibration mode shapes

$\nu$	$\text{Im}\lambda_\nu$ [Hz]	Dominant vibrations of bogie components accordant with mode shapes
1	1.262	vertical of CB in phase with BF and TMs of both IDs
2	2.694	torsion of TM rotor of ID1 with gear transmission, twisting of disc clutch
3	5.425	torsion of both gears and BF pitch, gearing deformations
4	5.449	vertical of BF with both TMs in phase
5	6.176	lateral and roll of BF with both TMs in phase
6	8.503	lateral of both TMs in opposite phase
7	8.584	combined longitudinal-pitch of W2 and combined BF roll-pitch
8	9.183	combined longitudinal-pitch of W1 and combined BF roll-pitch
9	12.208	combined longitudinal-yaw of W2
10	12.580	combined longitudinal-yaw of W1
58	298.4	torsion of ID1 pinion gear, twisting of ID1 driving shaft

BF... bogie frame  
 CB... car body  
 TM... traction motor  
 W1... wheelset of ID1  
 W2... wheelset of ID2



These values describe the possible operational state of the particular electric locomotive at the instant of the sudden short-circuit [4]. The first ten pairs of complex conjugate eigenvalues sequenced according to magnitude of imaginary parts and ten real eigenvalues sequenced from smallest values is presented in Table 1. Vibration mode shapes, corresponding to complex conjugate eigenvalues for  $s_0 = 0.005$ , are characterized in Table 2 in agreement with dominant vibrations and deformations of bogie components. Aperiodic mode shapes, corresponding to negative real eigenvalues, have no importance for dynamic load. Positive real parts of eigenvalues reflect system instability. This instability corresponding to positive real part of the complex conjugate eigenvalues is flutter type (see five eigenvalues for  $s_0 = 0.014$  in Table 2) and instability of a divergence type corresponds to real eigenvalues (see the first and second real eigenvalues for  $s_0 = 0.014$ ). Obviously the system is stable for longitudinal creepage  $s_0 = 0.005$  and unstable for large creepage  $s_0 = 0.014$ .

As an illustration, we present the dependence of real and imaginary parts of eight lowest eigenvalues on the longitudinal creepage  $s_0$  for the vehicle velocity  $v = 120$  km/h in Fig. 6. The stability limit for  $v = 120$  km/h is defined by creepage  $s_0 = 0.0082$ . We take a note that for higher vehicle velocity the limiting creepage is smaller (for  $v = 200$  km/h  $s_0 = 0.0069$ ).

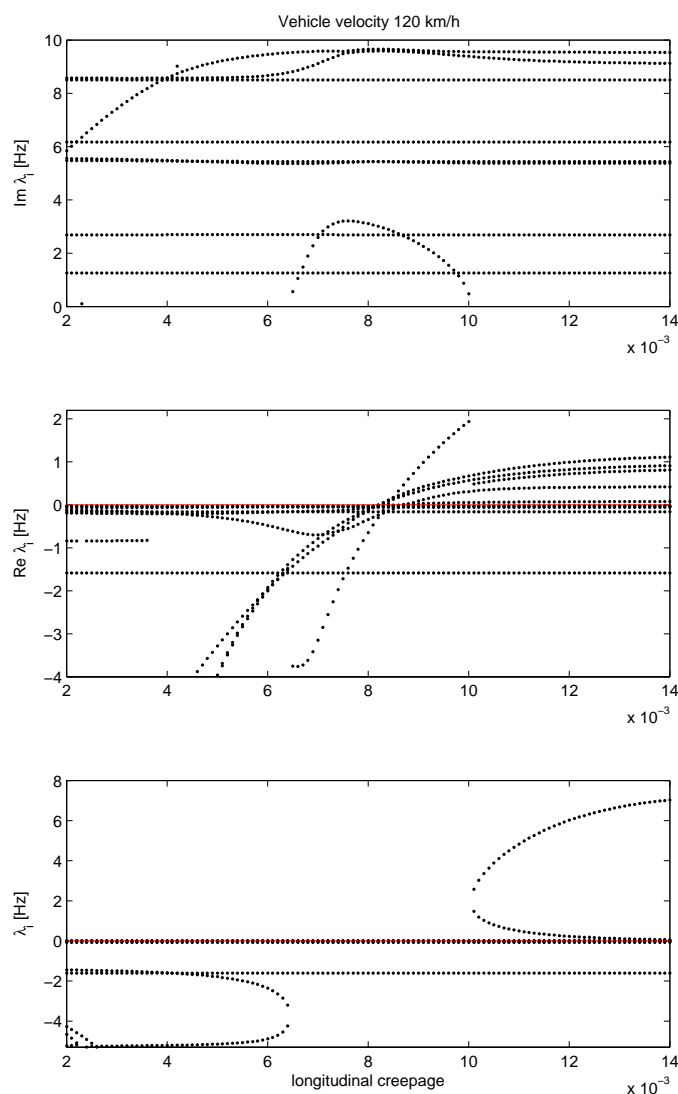


Fig. 6. Dependence of the imaginary parts (top), real parts (mid) of complex conjugate eigenvalues and real eigenvalues (bottom) on longitudinal creepage  $s_0$

### 5. Dynamic response caused by short-circuit motor torque

The short-circuit motor torque in the air-space of the particular traction motor was calculated in ŠKODA ELECTRIC, a. s., in dependence on time [4]. This dependence can be well approximated in perturbation coordinates of the model (20) by function (Fig. 7)

$$M_C(t) = -M(s_0, v)H(t) - M_0e^{-D\omega t} \sin[\omega(t - \Delta t)], \quad (23)$$

where  $M(s_0, v)$  is the traction motor torque in a state of the static equilibrium just before short-circuit,  $H(t)$  is Heaviside function and the oscillating short-circuit torque is defined by amplitude  $M_0$ , frequency  $\omega$ , shift phase  $\omega\Delta t$  and short-circuit torque decay  $D\omega$ . The total motor torque after short time (here 0.2 [s]) is equal zero (in perturbation coordinates is  $-M(s_0, v)$ ).

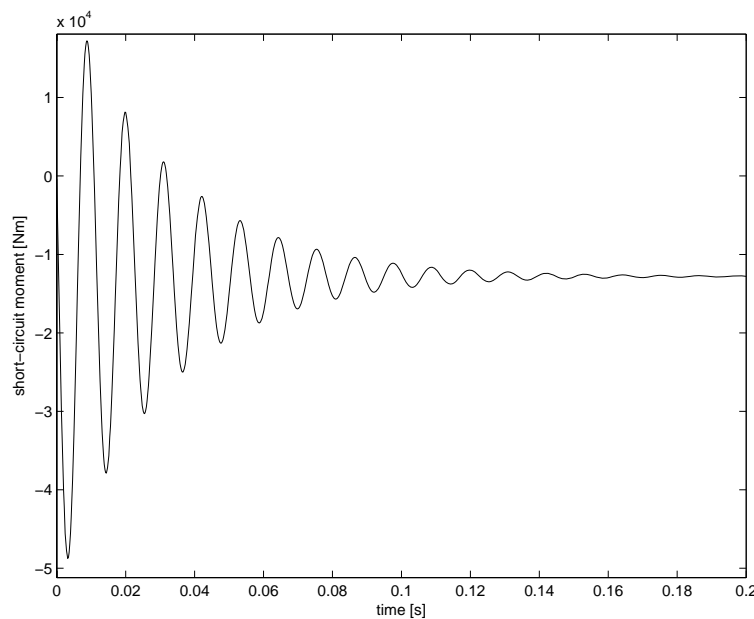


Fig. 7. Function approximating the disturbance by short-circuit moment in ID1

As an illustration the time behaviour in interval  $t \in \langle 0; 2 \rangle$  [s] of the dynamic torques and forces transmitted by chosen linkages of the wheelset drive of ID1 for operational parameters  $s_0 = 0.005$  and  $v = 120$  km/h at the instant of the short-circuit are presented in Fig. 8 to Fig. 10.

The frequency  $f = \omega/2\pi = 90$  [Hz] of the oscillating short-circuit torque and eigenfrequencies  $f_2 = 2.69$  [Hz] and  $f_{58} = 298.4$  [Hz], corresponding to mode shapes (see Table 2) characterized by torsion deformation of the flexible disc clutch ( $f_2$ ) and driving shaft ( $f_{58}$ ), show up as dominant. The identical values of the wheelset drive of ID2 are multiple smaller. The short-circuit motor torque causes an extreme load of the driving shaft torque  $M_{DS}$  approximately 50 % of its maximal value in time 0.18 [s] (Fig. 8). Maximal disc clutch torque  $M_{xDC}$  in the same time is cca  $10^5$  [Nm] (Fig. 9) which means greater value than the maximal adhesion wheelset moment  $M_{ad} = 2N_0r\mu_{\max}(v) = 0.52 \cdot 10^5$  [Nm] for  $v = 120$  [km/h].

Fundamentally worseness arises in the event of the short-circuit at large longitudinal creepage in the downward section of the creep characteristic (see Fig. 5). As an illustration the time behaviour of the driving shaft torque  $M_{DS}$  and of the disc clutch torque is shown in Fig. 11 for operational parameters  $s_0 = 0.014$  and  $v = 120$  [km/h] at the moment of the short-circuit. This model example illustrates relationship between modal properties and dynamic response of

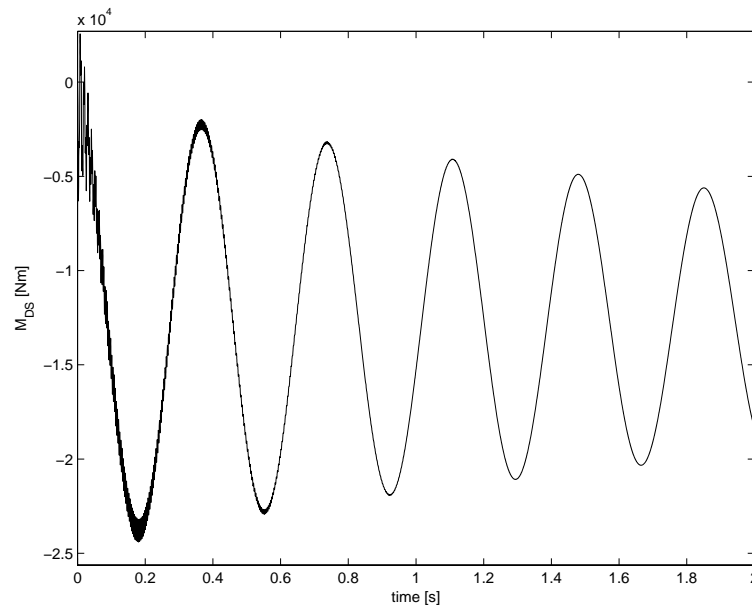


Fig. 8. Driving shaft torque

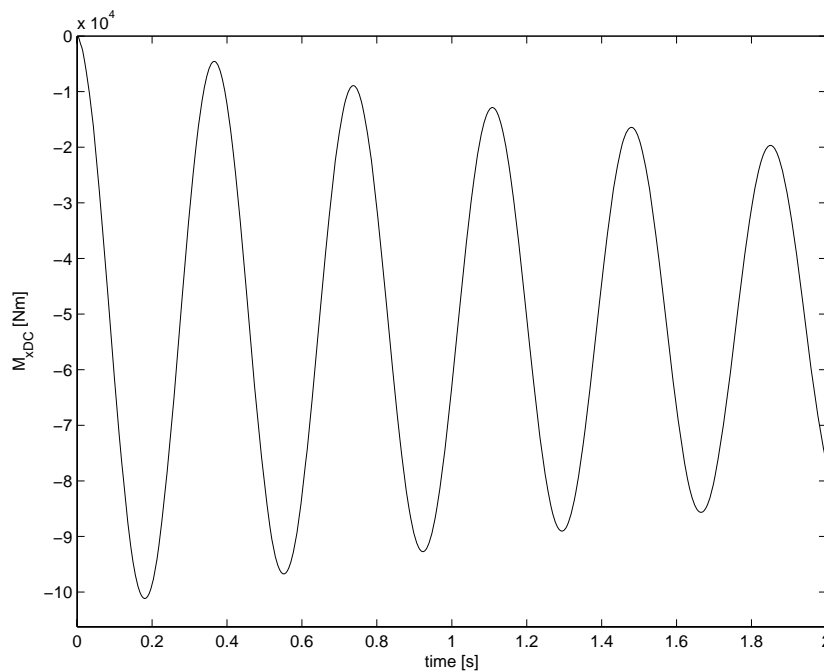


Fig. 9. Disc clutch moment

the unstable system and at once gives account of failure cause experimentally evidenced during testing operation of the real railway vehicle. Such large longitudinal creepage occurs e.g. in the case of a wet or a contaminated face of the rail. In consequence of system instability (real parts of five complex conjugate eigenvalues and two real values are positive – see Table 1) the both above-mentioned torques continuously increase until the antislip protection equipment is activated. The activation time should not be greater than cca 0.35 [s].

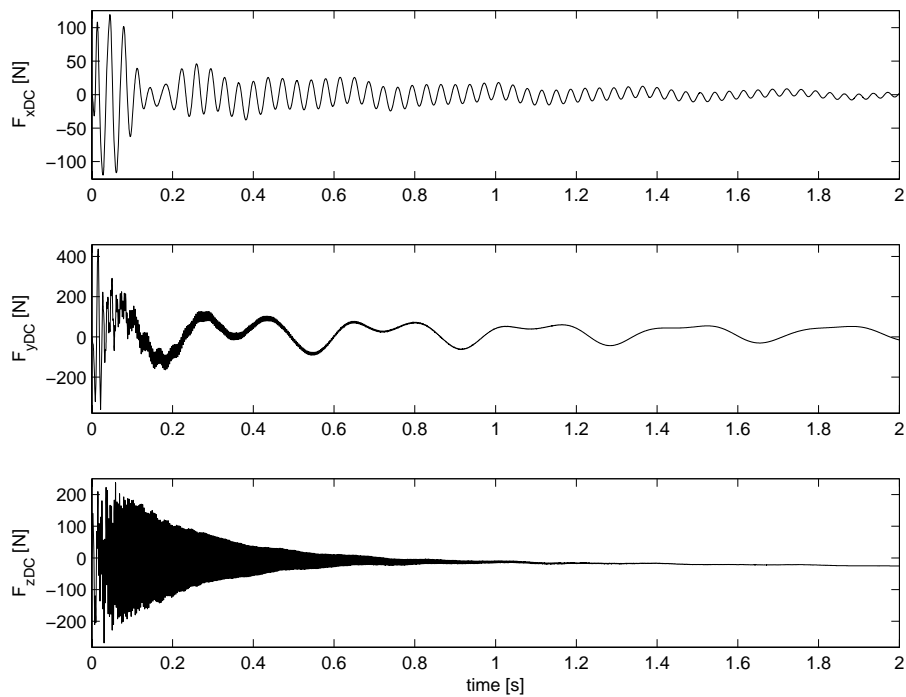


Fig. 10. Components of force transmitted by disc clutch

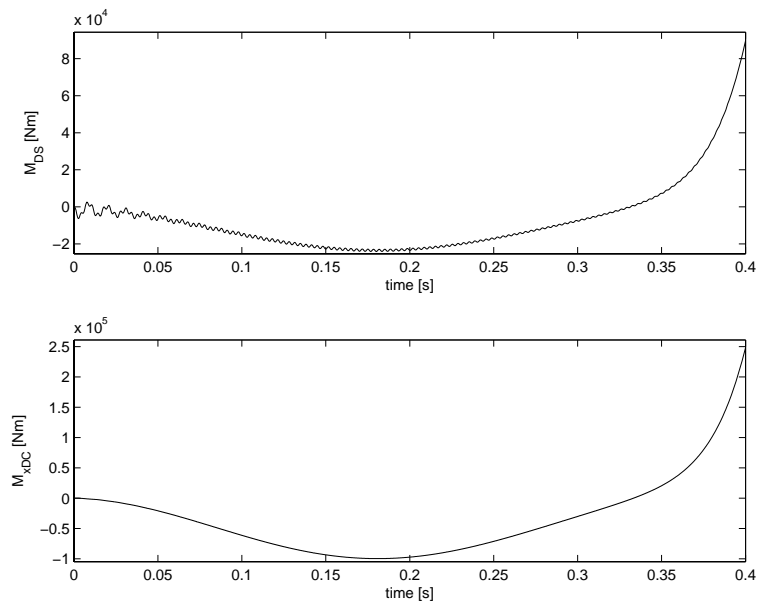


Fig. 11. Driving shaft torque (top) and disc clutch torque (bottom) caused by short-circuit moment in ID1 in unstable state ( $s_0 = 0.014$ ;  $v = 120$  km/h)

## 6. Conclusion

The paper presents the original mathematical modelling method and computer simulation of dynamic load of the wheelset drive caused by short-circuit motor moment. The detailed complex model of the railway vehicle bogie with two individual wheelset drives was used for studying of this extreme phenomenon. The model respects spatial vibrations of the traction motors, gear housings, hollow shafts, wheelsets, bogie frame and viscoelastic coupling among bogie components and among wheel rims and wheel discs, respectively. The mass, stiffness and damping of the rail ballast and the longitudinal, lateral and spin linearized creep forces in wheel-rail contacts are respected.

The dynamic response of the wheelset drive depends strongly on longitudinal creepage of wheels while on the forward locomotive velocity at the moment of the short-circuit has insignificant influence. In the event of the short-circuit in one traction motor at large longitudinal creepage the dynamic load of this wheelset drive extremely increases until activation of the antislip protection. The dynamic load of the normally working wheelset drive is low.

The developed software in MATLAB code enables graphically record time behaviour of the arbitrary generalized coordinates and with small software modification also the arbitrary forces transmitted by linkages between bogie components.

### Acknowledgements

This paper includes partial results from the Research Project MŠMT 1M0519 – Research Centre of Rail Vehicles supported by the Czech Ministry of Education, Youth and Sports.

### References

- [1] Byrtus, M., Zeman, V., Hlaváč, Z., Modelling and modal properties of an individual wheelset drive of a railway vehicle, *Sborník XVIII. mezinárodní konference Súčasný problémy v kolajových vozidlách – PRORAIL2007*, Žilina.
- [2] Claus, H., Schiehlen, W., System Dynamics of Railcars with Radial and Laterelastic Wheels, in *System Dynamics and Long Term Behaviour of Railway Vehicles, Track and Subgrade* (K. Popp and W. Schiehlen eds.), Springer, 2003, p. 65–84.
- [3] Čáp, J., Some aspects of uniform comment of adhesion mechanism, *Proceedings of VŠCHT Pardubice works*, 1993, p. 26–35 (in Czech).
- [4] Dvořák, P., Calculated values of the short-circuit moment in the air-space of the traction motor ML 4550 K/6, *Documentation of ŠKODA ELECTRIC, a.s., Plzeň*, 2009.
- [5] Feldman, V., Kreuzer, E., Pinto, F., Schlegel, V., Monitoring the dynamic of railway track by means of the Karhunen-Loeve-transformation, in *System Dynamics and Long Term Behaviour of Railway Vehicles, Track and Subgrade* (K. Popp and W. Schiehlen eds.), Springer, 2003, p. 231–246.
- [6] Fleiss, R., Laufverhalten des quergefederten Tatzlagerantriebs, *ZEVrail Glasers Annalen* 130 (6,7) (2006) 264–269.
- [7] Grag, V., Dukkipati, R., *Dynamics of railway vehicle systems*, London Academic Press, 1984.
- [8] Hlaváč, Z., Zeman, V., Optimization of the railway vehicle bogie in term of dynamic, *Applied and Computational Mechanics*, 1 (3) (2009) 39–50.
- [9] Jöckel, A., Aktive Dämpfung von Ratterschwingungen in Antriebstrang von Lokomotive mit Drehstrom-Antriebstechnik, *ZEV + DET Glas. Ann.*, 125 (5) (2001) 191–204.
- [10] Knothe, K., Systemdynamik und Langzeitverhalten von Shienenfahrzeugen, *Gleis und Untergrund*, *ZEVrail Glasers Annalen* 131 (4) (2007) 154–168.
- [11] Lata, M., Modelling of transient processes in torsion drive system of railway vehicle, *Scientific Papers of the University of Pardubice, Series B*, 2003, p. 45–58 (in Czech).
- [12] Lata, M., Dynamic processes in electric locomotive drive on rise of the wheelset slip, *Book of Extended Abstracts of the Conference Engineering Mechanics 2004*, Svratka, p. 165–166, (full paper on CD-rom).
- [13] Popp, K., Schiehlen, W. (Eds.), *System Dynamics and Long-Term Behaviour of Railway Vehicles, Track and Subgrade*, Springer-Verlag, 2003.
- [14] Zeman, V., Hlaváč, Z., Byrtus, M., Modelling of wheelset drive vibration of locomotive 109E, *Research report n. H2,H6-06-01/2006*, Research Centre of Rail Vehicles, Plzeň, 2007 (in Czech).
- [15] Zeman, V., Hlaváč, Z., Byrtus, M., Modelling and modal properties of the railway vehicle bogie with two individual wheelset drives, *Applied and Computational Mechanics*, 1 (1) (2007) 371–380.